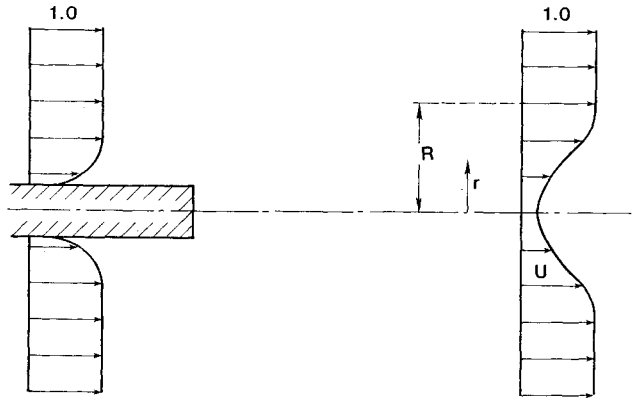

Fig. 1 Dimensionless velocity profiles in constant pressure regions.

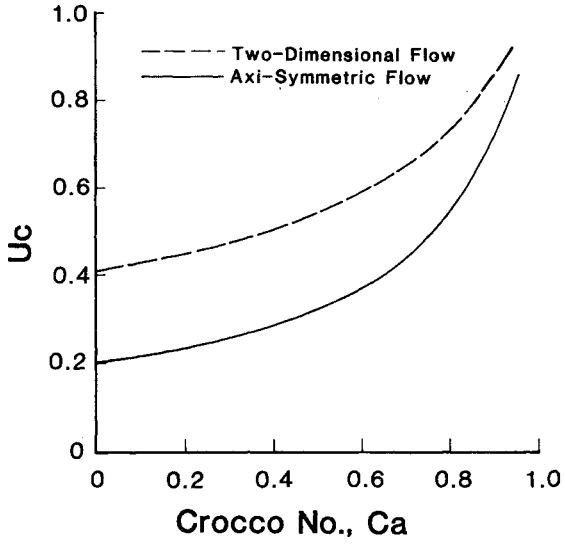

Fig. 2 Dimensionless centerline velocity vs Crocco number.

One version of the unified principle of thermodynamics[1] or the Second Law of Thermodynamics[2] is that the final equilibrium state of an isolated system is the state with maximum entropy. This principle can be applied to the near wake and has been useful in selecting one possible equilibrium state from a large number of choices in solving axisymmetrical wake problems.[3-5]

If a control volume is placed around the flow shown in Fig. 1, such that the outer control surface is in a constant pressure region parallel to the centerline, the dimensionless entropy flux from the control volume can be evaluated for a perfect gas at the constant pressure present in the control surface. The dimensionless entropy flux is represented by Eq. (2) for the axisymmetrical case where the flow is turbulent and the Reynolds number is very large:

$$\Sigma_{AS} = \int_0^1 \frac{\rho}{\rho_a}\frac{u}{u_a}\ell n\left(\frac{\rho_a}{\rho}\right)\left(\frac{r}{R}\right)\mathrm{d}\left(\frac{r}{R}\right) \tag{2}$$

Here, ρ is made dimensionless by the undisturbed adjacent density.

For the two dimensional case without dominant vortex shedding, the dimensionless entropy flux is shown by Eq. (3). Again, this is restricted to a case of turbulent flow with high Reynolds number in order that the effects of body boundary layer are negligible:

$$\Sigma_{2D} = \int_0^1 \frac{\rho}{\rho_a}\frac{u}{u_a}\ell n\left(\frac{\rho_a}{\rho}\right)\mathrm{d}\left(\frac{y}{Y}\right) \tag{3}$$

If one uses Eq. (1) for the near wake veloicty profile and a turbulent Prandtl number of unity in order that Eq. (4) can represent the density profile,[6] then the values of the near wake centerline velocity which maximizes Eqs. (2) and (3) can be determined. The results of these calculations are shown in Fig. 2.

$$\frac{\rho}{\rho_a} = \frac{1-C_a^2}{1-(u^2/u_a^2)C_a^2} \tag{4}$$

where

$$C_a^2 = (u_a^2)/(u_{\max}^2) = M_a^2/[M_a^2 + (2/k-1)] \tag{5}$$

Conclusion

Figure 2 presents the centerline velocity values which provide the most probable equilibrium solution. If one chooses to use a different but appropriate model for the near wake velocity profile or to account for Prandtl numbers different than unity, one will obtain slightly different numerical results. But, the important conclusion of the Note is that there exists a unique value of the time averaged centerline velocity in the near wake of a symmetrical body as a limiting case for turbulent high Reynolds number flow.

Acknowledgment

This material is based upon work partially supported by the National Science Foundation under Grant CBT-8418493.

References

[1]Hatsopoulous, G. N. and Keenan, J. H., *Principles of General Thermodynamics*, Wiley, New York, 1965.

[2]Kestin, J., *A Course in Thermodynamics—Vol. II*, Blaisdell, Waltham, MA, 1968.

[3]Page, R. H., "Subsonic Turbulent Base Drag," *Proceedings of the 14th Southeastern Seminar in Thermal Sciences*, North Carolina State Univ., Raleigh, NC, April 1978, pp. 348-363.

[4]Page, R. H., "Calculation of Turbulent Axisymmetric Subsonic Bluff Body Wakes with Influence of Mass Transfer," *Symposium on Turbulent Shear Flow*, Imperial College, London, England, July 1979.

[5]Page, R. H., "Compressible, Subsonic, Axisymmetric Base Flows," *Proceedings of Symposium on Rocket/Plume Fluid Dynamic Interactions*, Army Research Office, Research Triangle, NC, April 1983.

[6]Korst, H. H., "Auflösung eines ebenen Freistrahlrandes bei Berücksichtigung der ursprünglichen Grenzschichtströmung," Österreichisches Ingenieur-Archiv, Vol. 7, No. 2, March 1954.

Shock Wave Formation in a Suddenly Compressed Rubber Rod

G. Mazor,* G. Ben-Dor,† M. Mond,‡ and O. Igra§
Ben-Gurion University of the Negev
Beer Sheva, Israel

Received Sept. 3, 1986; revision received March 13, 1987.

*Ph.D. Student, Department of Mechanical Engineering, Pearlstone Center for Aeronautical Engineering Studies.

†Associate Professor, Department of Mechanical Engineering, Pearlstone Center for Aeronautical Engineering Studies.

‡Senior Lecturer, Department of Mechanical Engineering.

§Professor, Department of Mechanical Engineering, Pearlstone Center for Aeronautical Engineering Studies.

Introduction and Definition of the Problem

CONSIDER Fig. 1a, where an incident shock wave propagates from left to right inside a shock tube toward a plate having the same cross section. The plate, which is free to move along the tube, is supported by a rubber rod that has a smaller cross section and is free to expand both in the y and z directions. Before the incident shock wave collides head-on with the plate, the rubber rod, which is free of any internal stresses, has an initial length L_0. The flow states ahead of and behind the incident shock wave are 1 and 2, respectively. Upon colliding with the plate, the incident shock wave is reflected backwards, generating behind it a high-pressure zone, state 5. The sudden rise of the pressure from p_1 to p_5 on the left side of the plate accelerates it from left to right. The acceleration of the plate will trigger two waves, a rarefaction wave to the left and a compression wave to the right (Fig. 1b). The rarefaction wave propagates into state 5 while reducing the pressure acting on the plate to p_6. The compression waves propagates into the rubber rod and compress it. The question to be answered in this Note is, where will the compression waves converge into a shock wave along the rubber rod?

Present Study

The approach to solving this problem is similar to that used for calculating the location where the compression waves (generated by an accelerating piston in a gas) converge into a shock wave. Consider Fig. 1c, where a schematical illustration of the compression wave in the rubber rod is shown in the (x,t) plane together with the trajectory of the plate. At $t=0$, when the plate starts accelerating, the head of the compression wave C_0 starts moving into the rubber rod. It is immediately followed by other compression waves that are generated as long as the plate accelerates. In Fig. 1c, only the second compression wave, C_1, is illustrated. It is generated at time t_ϵ when the plate reaches a distance x_ϵ; i.e., the rubber rod has been compressed from its initial length L_0 to a shorter length $L_0 - x_\epsilon$. At a time t_s, the second compression wave overtakes the first one, forming a shock wave at x_s. Thus in order to calculate x_s and t_s one must develop expressions for the velocities of the first and second compression waves and intersect their trajectories while requiring that $t_\epsilon \to 0$. It should be noted that the previously mentioned compression waves are known in the literature as Riemann waves.

The velocity at which a longitudinal disturbance is transferred from one particle to another in a solid medium with respect to the moving solid particles (i.e., Riemann waves) is[1]

$$g_n = \left[\frac{1}{r_0}\frac{\partial \sigma_n}{\partial \lambda}\right]^{1/2} \tag{1}$$

where r_0 is the density of the solid medium, σ_n the stress, and λ the strain.

Two cases will be evaluated herein, namely, a rubber rod under a one-dimensional compression (i.e., free to expand in the y and z directions) and a rubber rod under a two-dimensional compression (i.e., free to expand in the z direction only). The index n in the following expressions should assume the value of 1 for the one-dimensional compression case and value of 2 for the two-dimensional compression.

The stress-strain relation for a rubber under compression is[2]

$$\sigma_n = G_n[\lambda - (1/\lambda^{n+1})] \tag{2}$$

where G_n is a constant defining the elasticity of the rubber. Nowinski[3] showed that the absolute velocity of the Riemann waves with respect to an inertial frame of reference is

$$C_n = V + \lambda g_n \tag{3}$$

where V is the absolute velocity of the solid particles.

Inserting Eqs. (1) and (2) into Eq. (3) results in

$$C_n = V + \left(\frac{G_n}{r_0}\right)^{1/2}\left(\lambda^2 - \frac{n+1}{\lambda^n}\right)^{1/2} \tag{4}$$

Equation (4) indicates that the absolute velocity of the particles, V, must be known in order to evaluate the absolute velocity of the Riemann waves.

In the following paragraphs, an expression for V will be developed. The expression is developed for a small time interval following the head-on collision, i.e., $0<t<t_\epsilon$ where $t=0$ is the collision time and $t_\epsilon \to 0$.

The equation of motion of the plate supported by the rubber rod after the head-on collision of the incident shock wave is

$$\frac{d}{dt}\{[m+M(t)]\dot{x}\} = p_6(t)A_s + \sigma_n(t)A_R \tag{5}$$

where m is the mass of the plate; $M(t)$ the mass of the rubber particles which have been accelerated during the time t; A_s and A_R the cross sections of the plate and the rubber rod; respectively; $\sigma_n(t)$ the stress inside the rubber rod (negative for this case of compression), and $p_6(t)$ the gas pressure (behind the rarefaction wave) acting on the left side of the plate. Since state 6 is connected to state 5 through a rarefaction wave (Fig. 1b),[4]

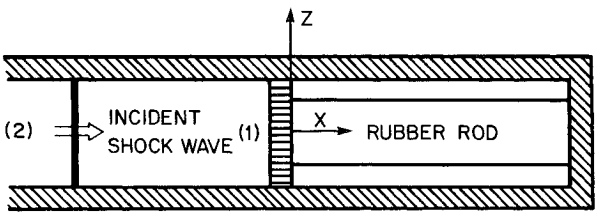

Fig. 1a Schematic of the rubber rod prior to the head-on collision.

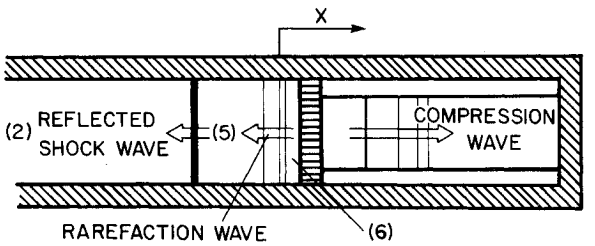

Fig. 1b Schematic of the waves system after the head-on collision.

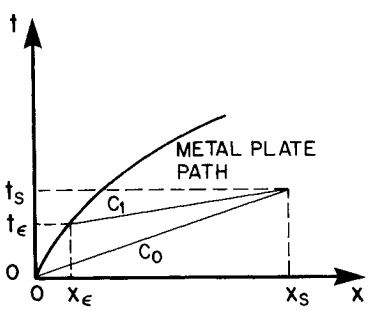

Fig. 1c Schematic of the first and second Riemann waves trajectories in the (x,t) plane. Note $t=0$ corresponds to the moment when the incident shock wave collided head-on with the plate.

$$p_6(t) = p_5\left[1 - \frac{u_6(t)(\gamma-1)}{2a_5}\right]^{2\gamma/(\gamma-1)} \tag{6}$$

but $u_6(t)$, the particle velocity in state 6 is identical to the plate velocity and hence $u_6(t) = \dot{x}(t)$. The strain λ can also be expressed in terms of x through the following relation $\lambda = L/L_0 = 1 - x/L_0$, where L_0 is the initial length of the rubber rod. Inserting the preceding relation into Eq. (5) and assuming that during the short time interval $0 < t < t_\epsilon$, 1) the pressure acting on the left side of the plate remains practically constant, and 2) the mass of the rubber particles being accelerated is negligibly small compared to the mass of the plate, resulting in

$$\ddot{x} + \omega_n^2 x = \frac{P_5 A_s}{m} \tag{7}$$

where

$$\omega_n = \left[\frac{(n+2)G_n A_R}{L_0 m}\right]^{1/2}$$

defining

$$K_n = \left[\frac{(n+2)G_n A_R}{L_0}\right]$$

gives

$$\omega_n \left(\frac{K_n}{m}\right)^{1/2}$$

For the initial conditions $x(t=0) = 0$ and $\dot{x}(t=0) = 0$, Eq. (7) results in

$$x = B_n(1 - \cos\omega_n t) \tag{8}$$

where

$$B_n = \frac{P_5 A_s}{K_n}$$

Thus the velocity of the rubber particles that are adjacent to the plate is

$$V = \dot{x} = B_n \omega_n \sin\omega_n t \tag{9}$$

Inserting Eq. (9) into Eq. (4) finally results in the velocity of the Riemann waves

$$C_n = B_n \omega_n \sin\omega_n t + \left(\frac{G_n}{r_0}\right)^{1/2}\left(\lambda^2 + \frac{n+1}{\lambda^n}\right)^{1/2} \tag{10}$$

Consider again Fig. 1c, where the first two Riemann waves C_0 and C_1 are shown. The velocity of the first Riemann wave C_0 can be obtained from Eq. (10) by inserting $t = 0$ and $\lambda = 1$ (i.e., $x = 0$):

$$(C_0)_n = \left[\frac{(n+2)G_n}{r_0}\right]^{1/2} \tag{11}$$

Note that the value of C_0 as obtained from Eq. (11) agrees with that quoted in the literature, since from Eq. (2) one can get

$$E_n = \left.\frac{\partial \sigma_n}{\partial \lambda}\right|_{\lambda=1} = (n+2)G_n$$

Thus Eq. (11) assumes the well-known expression[5]

$$(C_0)_n = \left(\frac{E_n}{r_0}\right)^{1/2} \tag{12}$$

It should be noted that the expression for $(C_0)_n$ as obtained form Eq. (12) is identical for elastic linear materials for which the Young modulus E is constant. Thus, as can be expected, for small strains the rubber can be assumed to satisfy Hook's law. It should also be noted that in the case of a rubber, $(C_0)_n$ as calculated from Eq. (12) is about 46 m/s. In metals, however, such as steel, copper, and aluminum, the values of C_0 are 5940, 4560, and 6320 m/s, respectively. The relatively low value of $(C_0)_n$ enables a shock wave to be formed quite easily in rubbers, while in metals, where the value C_0 is so high, a shock wave can be formed only in the plastic range.

The second Riemann wave C_1 is generated at $t = t_\epsilon$ when the rubber rod is compressed by $x = x_\epsilon$, i.e., $\lambda = 1 - (x_\epsilon/L_0)$. From Eq. (8),

$$x_\epsilon = B_n(1 - \cos\omega_n t_\epsilon) \tag{13}$$

Thus the velocity of the second Riemann wave is

$$(C_1)_n = B_n\omega_n \sin\omega_n t_\epsilon + \left(\frac{G_n}{r_0}\right)^{1/2}\left[1 + \frac{B_n}{L_0}(\cos\omega_n t_\epsilon - 1)\right]^2 + 2\left[1 + \frac{B_n}{L_0}(\cos\omega_n t_\epsilon - 1)^{-1}\right]^{1/2}$$

The distances travelled by the first and second Riemann waves are $x = (C_0)_n t$ and $x = x_\epsilon + (C_1)_n(t - t_\epsilon)$, respectively.

As mentioned earlier, a shock wave is generated at the place where the second Riemann wave overtakes the first one. This point, shown as x_s in Fig. 1c, can be obtained by intersecting the previous expressions, i.e.,

$$(x_s)_n - (C_0)_n \frac{(C_1)_n t_\epsilon - x_\epsilon}{(C_1)_n - (C_0)_n}$$

Inserting $(C_0)_n$, $(C_1)_n$, and x_ϵ into the preceding expressions and solving for the limit $x_\epsilon \to 0$ yields

$$(x_s)_n = \frac{(C_0)_n}{B_n\omega_n^2}\left[\frac{(n+2)G_n}{r_0}\right]^{1/2}$$

which by inserting B_n and ω_n becomes

$$(x_s)_n = \frac{(C_0)_n^2 m}{P_5 A_s} \tag{14}$$

Two-Dimensional Compression

Consider again Fig. 1a and assume that the rubber rod extends from one side of the shock tube to the other in the y direction (perpendicular to the page) and hence can freely expand only to the z direction, i.e., $\sigma_z = 0$. For this case, known as two-dimensional compression,[2]

$$\sigma_x = \frac{2}{\lambda_x}(\lambda_x^2 - \lambda_z^2)(A_1 + A_2\lambda_y^2) \tag{15}$$

Treloar[2] showed experimentally that

$$A_1 = 1.6 \text{ kgf/m}^2 \text{ and } 0.05 < A_2 < 0.3 \text{ kgf/m}^2$$

Since the rubber rod cannot expand in the y direction, $\lambda_y = 1$. Furthermore, if we assume that the rubber is incompressible, then[2] $\lambda_x \lambda_y \lambda_z = 1$. Inserting $\lambda_y = 1$ into this expression gives $\lambda_z = 1/\lambda_x$. Inserting the last expression into Eq. (15) and replacing λ_x and σ_x by λ and σ_2 respectively results in

$$\sigma_2 = (A_1 + A_2)\left(\lambda - \frac{1}{\lambda^3}\right) \tag{16}$$

which satisfies Eq. (2) if one defines $G_2 = (A_1 + A_2)$. The remaining development for two-dimensional compression is identical to the one given earlier with $n = 2$ rather than $n = 1$, which gives the appropriate expressions for a one-dimensional compression.

Discussion and Conclusions

The location along a rubber rod where the compression wave generated upon an impact on one of its edges has been calculated for one- and two-dimensional compression. The case of a three-dimensional compression could not be solved due to lack of an expression relating the stress to the strain.

Comparing Eq. (12) for $n = 1$ and $n = 2$ by calculating the velocity of the first Riemann wave (the values of the various physical constants are taken from Ref. 5) indicates that for a one-dimensional compression,

$$(C_0)_1 = 46.37 \text{ m/s}$$

while for a two-dimensional compression

$$26.37 < (C_0)_2 < 28.29 \text{ m/s}$$

where the lower and upper limits correspond to the smaller and higher values of A_2 respectively. Thus, as can be seen, the first Riemann wave, i.e., the velocity and the head of the compression wave in a two-dimensional compression, travels at about 60% the velocity of the head of the compression wave in the case of a one-dimensional compression. This suggests that for the same impact conditions, a shock wave will be formed much earlier when the rubber rod can expand only in one direction.

From Eq. (14) one can get

$$\frac{(x_s)_2}{(x_s)_1} = \left[\frac{(C_0)_2}{(C_0)_1}\right]^2$$

and since $(C_0)_2 \approx 0.6(C_0)_1$ one obtains $(x_s)_2 \approx 0.36(x_s)_1$, which means that the distance where a shock wave is formed in a rubber rod under a two-dimensional compression is about one-third the distance needed for a shock wave to be formed when the rubber rod is only under a one-dimensional compression.

References

[1]Courant, R. and Friedricks, K. O., *Supersonic Flow and Shock Waves*, Vol. 1, Interscience Publications Inc., New York, London, 1948.

[2]Treloar, L. R. G., *The Physics of Rubber Elasticity*, Oxford at the Clarendon Press, Oxford, 1949.

[3]Nowinski, J. L., "On the Propagation of Finite Disturbances in Bars of Rubberlike Materials," *Journal of Engineering for Industry*, Vol. 87, 1965, pp. 523–529.

[4]Glass, I. I. and Hall, J. G., "Shock Tubes," *Handbook of Supersonic Aerodynamics*, Vol. 6, Sec. 48, NAVORD Rept. 1488, 1959.

[5]Kolsky, H., *Stress Waves in Solids*, Dover Publications Inc., New York, 1952.

Hybrid Finite-Element Analysis of Laplace's Equation with Singularities

Kuen Ting* and Wen-Hwa Chen†
National Tsing Hua University, Hsinchu, Taiwan

Introduction

THIS Note is devoted to solving Laplace's equation subjected to appropriate boundary conditions with singularities. Earlier attempts to solve this problem using finite-element techniques used conventional elements[1] or quarter-point singular elements.[2,3] Although those elements were easily used in available finite-element packages, a rather refined mesh needed to be employed. Several investigators[4,5] then created a special singular element to model the region near the singular point, but did not satisfy the condition of continuity for the independent variables in partial differential equations. Recently, the global element method[6,7] for which shape functions with an embedded singularity have been devised for this problem with relatively simple domains (e.g., circles, squares, etc.). Thus, it would be preferable to construct a finite-element model that can be used to solve the Laplace equation with complicated geometries such that singularities are considered in several special elemens surrounding the singular point and conditions of continuity of solutions at the interelement boundaries are still satisfied. The hybrid finite-element models developed by the authors[8,9] in dealing with thermoelastic fracture problems seem to be good choices for this purpose.

Motz's Problem

As shown in Fig. 1, without loss of generality, the problem first introduced by Motz[10] is chosen as the example to tackle: The problem is governed by the two-dimensional Laplace equation

$$\nabla^2 u = 0 \text{ in R}$$

subjected to the boundary conditions

$$u = f_1 \text{ on OP}$$

$$= f_2 \text{ on BC}$$

and

$$\frac{\partial u}{\partial n} = g \text{ on AB, AD, CD}$$

where $\partial u/\partial n$ is the outward normal gradient of u, and f_1, f_2, and g are constants.

Hybrid Finite-Element Analysis

The variational principle that governs the hybrid finite-element models for thermoelastic fracture problems can be further generalized as follows:

$$\pi(u, \tilde{u}, \tilde{\lambda}_n) = \sum_m \left\{ \int_{A_m} \frac{1}{2} (\nabla u)^T (\nabla u) \mathrm{d}A + \int_{S_{hm}} g\tilde{u} \mathrm{d}s \right.$$

Received Nov. 13, 1986; revision received Feb. 18, 1987.

*Graduate Student, Department of Power Mechanical Engineering.

†Professor and Head, Department of Power Mechanical Engineering.